Hindawi
Mathematical Problems in Engineering
Volume 2018, Article ID 6583908, 8 pages
https://doi.org/10.1155/2018/6583908

Research Article

An Improved Genetic Algorithm to Optimize Spatial Locations for Double-Wishbone Type Suspension System with Time Delay

Qiang Li[1,2] **Xiaoli Yu**[3] **and Jian Wu**[1,2]

[1]*School of Mechanical & Automotive Engineering, Zhejiang University of Science and Technology, Hangzhou 310023, China*
[2]*Provincial Key Laboratory of Food Logistics Equipment & Technology, Zhejiang University of Science and Technology, Hangzhou 310023, China*
[3]*Power Machinery & Vehicular Engineering Institute, Zhejiang University, Hangzhou 310013, China*

Correspondence should be addressed to Qiang Li; liqiang1353@163.com

Received 17 June 2017; Accepted 10 October 2017; Published 20 February 2018

Academic Editor: Radek Matušů

By taking account of double-wishbone independent suspension with two unequal-length arms, the coordinate values of articulated geometry are based on structural limitations and constraint equations of alignment parameters. The sensitivities of front wheel alignment parameters are analyzed using the space analytic geometry method with insight module in ADAMS® software. The multiobjective optimization functions are designed to calculate the coordinate values of hardpoints with front suspension since the effect of time delay due to wheelbase can be easily obtained by vehicle speed. The K&C characteristics have been investigated using GA solutions in the simulation environment. The camber angle decreases from 1.152° to 1.05° and toe-in angle reduces from 1.036° to 0.944°. The simulation results demonstrate that the suggested optimization method is able to satisfy the suspension motion to enhance ride comfort. Experimental results, obtained by K&C test bench, also indicate that the optimized suspension can track the desired trajectory while keeping the vehicle performance in various road conditions.

1. Introduction

Modern automotive engineers have paid more and more attention to the suspension system almost as soon as they were always concerned about automotive performance parts and accessories more than power and acceleration [1, 2]. To correspond with the increased demand for suspension system, various optimization methods have penetrated into the practical application over the last two decades [3–7]. The purpose of suspension with flexibly connecting the wheels to the vehicle frame is to provide good handling and harshness with steering stability to ensure the passengers comfort while maximizing the friction between the tires and road surface.

The suspension guides respective up-and-down wheel motions by actuating two wishbone-shaped control arms comprising six mounting positions and corresponding joints. There are three joints in individualistic control arm. The two joints link with the vehicle frame and the other joint connects with the wheel hub.

The coil springs and dampers (shock absorbers) are oriented along the bell crank through the pushrods or pullrods in view of the nonlinear time delay system. The spring and damper apparatus convert up-and-down wheel motions to back-and-forth movements that capture the lagged characteristics of road excitations.

Since the double-wishbone suspension as an important chassis part can rapidly deviate from its desired path, especially the widely used unequal length of upper and lower control arm (long short arm, LSA), the kingpin inclination, small delays, or lags can lead to deteriorating the real-time vehicle performance. The optimal solution of suspension parameters can be tuned to meet the scope of tread in alignment within acceptable limit levels. As a result, because of adjusting spatial locations in the unequal-length double-wishbone suspensions, the understeering/oversteering dynamics behaviors that express "pushing" or "loose" phenomenon of a vehicle vary widely with changes in various operating conditions. From sixteenth-century wagons to nowadays Formula one, a

wide range of studies that coordinates optimization method and nonlinear time delay system to enhance the ride and handling characteristics has been introduced.

Tak et al. [8] develop the kinematic static sensitivity equations to meet some prescribed performance targets during the whole optimization procedure. Suh et al. [9] conduct the influences of the change of rear suspension geometry to investigate the handling performances of a large-sized bus. Park et al. [10] discuss the ADAMS full vehicle model in driving condition based on the on-board measurements and transformation matrix. Kim et al. [11] examine effect on hands-free stability of steering and suspension design variables to prove their correlations with ADAMS/Car simulation methods. The numerical simulation models and optimal solution procedures have high degree of complexity. The sensitivity analysis has not been explicitly defined with high correlativity with suspension parameters. The shortcoming of traditional optimization algorithm has only one directional preset track.

The research results have also shown that several Genetic Algorithm (GA) control strategies [12–15] are extensively investigated in the development of linkage kinematics with optimal configuration in many commercial software programs, such as ADAMS and Visual C++. Mitchell et al. evaluate the impact of multiple independent metrics with the assistance of a user selectable weighting use of GA. Yan et al. [16] study GA-optimized fuzzy controller by means of MATLAB-ADAMS union simulation. The GA gives the best performances on each optimized circuit to fasten design processes and narrows and chooses the best one from alternate optimal solutions.

The paper is organized as follows. Section 2 defines novel design method of the double-wishbone type suspension. The quasi-static suspension models are evaluated using ADAMS. The sensitivity analyses are examined with several hardpoints. The binary string with certain design valuables considered as a chromosome is determined in Section 3.1 The comparison of dynamic wheel alignments with computation suspension and steering model and actual best bench are obtained in Section 3.4. Finally, we conclude that the validation of optimization method and procedure are presented to meet prescribed performance targets in Section 4.

2. Modelling and Static Analysis

2.1. Background for Suspension Model. The double-wishbone type suspension, known as an A-arm construction, is widely used for front *n* and rear axles with separate type steering trapezium, especially in mainstream larger cars and racing cars. The double-wishbone type suspension can easily modify the interaction between the tire and the road surface to achieve the improved maximum friction. The double-wishbone type suspension has proven itself as one of the effective mechanics that enhances the ride and handling ability to steer, brake, and accelerate. Meanwhile, it has advantages in the fact that it has contributed to elimination or minimization of lateral load transfer distribution for the sake of more consistent road feeling.

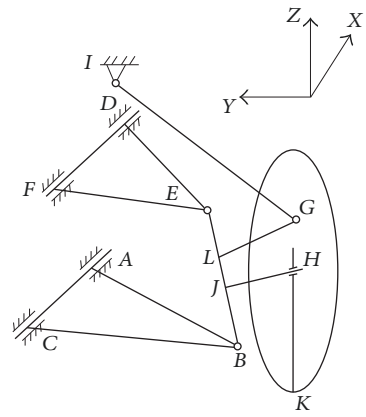

Figure 1: Schematic diagram of a front-right LSA suspension system and steering mechanism.

It is essential to design the hardpoint positions at the beginning stage through the Cartesian (absolute) coordinates in order to establish a unified standard for different work groups. The optimal method of rear hardpoint positions can be easily calculated by less constraint equations without considering the length of tie rod. The camber at steering knuckle position is designed to ensure symmetry and Ackermann geometry status during steering. Also it is a very different task for chassis assignment of checking movement interventions.

2.2. Structure of LSA Suspension. For the double-wishbone type suspension, tie rod is the line connecting two points of spherical joints *G* and *I* (rack and pinion type steering system); triangle DEF and ABC are composed of upper and lower control arm, which revolve about the *DF* axis and *AC* axis, respectively. *E* and *B* indicate upper and lower spherical joints to the steering knuckle, separately. The axes *GL* and *EB* separately represent the steering knuckle arm and steering axis inclination (SAI), also called kingpin inclination (KPI). The axis *JH* expresses the wheel linkage with kingpin. The *K* point can simplify to be regarded as contact point of wheel tread. As an example, a double-wishbone type front suspension system, as illustrated in Figure 1, is a combination of steering mechanism four degrees of freedom (DOF). Thus, constraint equations can be expressed before and after moving using initial points as rigid body motion.

The constrain equations of vertical relationships can be deduced by

$$\begin{aligned}(x_H - x_J)(x_K - x_H) + (y_H - y_J)(y_K - y_H) \\ + (z_H - z_J)(z_K - z_H) = 0.\end{aligned} \tag{1}$$

After LSA suspension moving, the new orientation of the ball joints (denoted by x', y', z') can be denoted based on the new location of SAI.

The constraint equations of constant distances can be written as

$$\begin{aligned}\Delta x, y, z = (x, y, z) - \left(x', y', z'\right), \\ l = \sqrt{(\Delta x)^2 + (\Delta y)^2 + (\Delta z)^2}.\end{aligned} \tag{2}$$

Table 1: Original design variables of hardpoint positions in front suspension system (mm).

Axis	*O*	*A*	*B*	*C*	*D*	*E*	*F*	*G*	*H*
x	0	−146.6	−10.2	126.3	−146.6	126.3	7.8	−70.0	0
y	0	196.2	571.2	196.2	261.5	555.2	261.5	571.2	622
z	0	−134.3	−129.3	−134.3	75.7	99.5	75.7	−100	0

The new locations of upper spherical joints connecting the steering knuckle can be expressed by

$$\begin{aligned} l_{EB} &= l'_{EB}, \\ l_{EF} &= l'_{EF}, \\ l_{ED} &= l'_{ED}. \end{aligned} \tag{3}$$

Similarly, the new positions G and H can be provided by

$$\begin{aligned} l_{EG} &= l'_{EG}, \\ l_{IG} &= l'_{IG}, \\ l_{BG} &= l'_{BG}, \\ l_{EH} &= l'_{EH}, \\ l_{BH} &= l'_{BH} \\ l_{GH} &= l'_{GH}. \end{aligned} \tag{4}$$

Constraint equations are solved for the corresponding locations of the lower and upper control arms using MATLAB.

To describe the three-dimensional kinematic model for suspension characteristics and wheel movements, the original hardpoint positions in the front-right LSA suspension system are listed in Table 1.

2.3. Dynamic Responses. The front LSA suspension is modelled using ADAMS as a multibody simulation tool [17]. The suspension consists of a Panhard bar to withstand the tire principal lateral force, an upper control arm, and a lower control arm which are subject to decomposing longitudinal driving, braking, and vertical forces. The steering system comprises a steering wheel, a steering column, pitman arm, rack, and pinion gearbox, as indicated in Figure 2. The distribution coefficient of the total weight can be optimized by adjusting mount positions and spring perches of control arms.

To compare the effects of different coordinate values of hardpoints, the dynamic responses of the LSA suspension are developed to evaluate the relationship between ride comfort and handling for specifying spring stiffness and damper rate under road load conditions. The dynamics ADAMS model that is integrated with steering system and suspension system expressed as boundary conditions are developed to compare the performances of current designs.

In static analysis, the wheel travel of LSA suspension is updated with a range from −30 mm to 30 mm to reflect

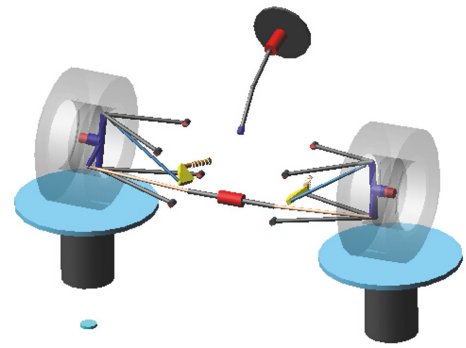

Figure 2: Simulation model of front suspension system and steering mechanism.

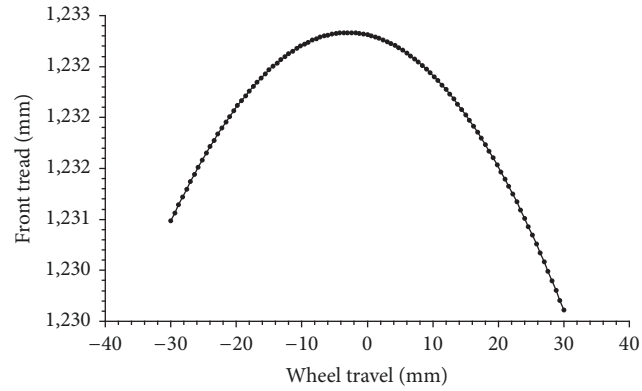

Figure 3: Variations of wheel travel related to front tire tread.

the changes of tread curve, as illustrated in Figure 3. Wheel travel measures use the following convention: positive values indicate compression motion, whereas negative displacement represents extension process. The simulation results reveal significant effect of wheel travel on tire tread. The larger the wheel travel along with up or down direction varies, the higher the change rate the tire tread generates is. The proposed positions of tie rod joint and length of steering pitman arm as important structural parameters distinguish the front suspension from the rear one considering spatial constraints and attribute constraints.

2.4. Sensitivity Analysis. The INSIGHT module from ADAMS finds the parameter sensitivity analyses that minimize the effects of road excitation or other disturbances upon the tires movement while satisfying the constraints on the double-wishbone type suspension geometry constraints. The suspension compliances are specified by variance functions that aim to describe the influence of the

Table 2: Sensitivity analysis of design variables, %.

Hardpoints	Toe	Camber	SAI	Caster
$y_A(x_1)$	−1.07	0.01	0.02	0
$z_A(x_2)$	−3.42	17.7	13.5	−1.16
$y_C(x_3)$	−1.08	0.01	0.01	0.01
$z_C(x_4)$	−2.96	17.41	13.65	0.68
$y_D(x_5)$	−0.26	−1.56	−1.61	0.42
$z_D(x_6)$	−0.68	−16.51	−16.84	1.01
$y_F(x_7)$	−0.22	−1.52	−1.61	−0.37
$z_F(x_8)$	−0.28	−16.1	−17.07	−1.97
$y_G(x_9)$	−1.32	−0.01	0	0
$z_G(x_{10})$	8.26	−7.6	0.15	0.15

coordinates of hardpoints during operations. The wheel geometry parameters that affect the steerability of the vehicle are camber, caster, SAI, and toe.

The sensitivity results of wheel geometry parameters can be calculated as the steering effort and steering wheel returnability produced by the tires to predict the behaviors of vehicle as shown in Table 2. The negative caster angles can reduce the steering effort but weaken the steering wheel returnability. Smaller SAI angles can be favourable to steering effort but deteriorate the steering wheel returnability as well. For that purpose, optimal approaches of design parameters changes used to require trade-offs to retain mutual balance. The sensitivity characteristics of different wheel alignment parameters are strongly correlated with hardpoint positions of control arms in the suspension system.

In Table 2, the different contributing levels of each hardpoint position have been revealed to their effects on the variations of wheel alignments. The SAI angle is mainly dependent on the vertical locations of A, C, Z, and F points; the toe angle depends on the vertical locations of A, C, and G points. The vertical locations of A, E, and F points as the design important parameters have a significant effect on camber angle on steering response. The data analysis of Table 2 allows us to explore potential of optimization of the locations of critical hardpoints with multiobjective function and geometry constraints.

3. Optimization and Simulation

3.1. GA Optimization Method. Genetic Algorithms as optimization techniques using powerful and global search methods imitate the processes present in natural evolution based on Darwinian's survival of the best fitness theory [18–21]. Three coral and repeating stages mainly consist of selection, crossover, and mutation. Therefore, the biological individuals contained in design variables as a population can be converted into one long informative string. It is a convenient way to regard binary segments encoding the optimal parameters as a chromosome. The convergence of population members is checked and updated at each time step after the evaluation of fitness. The fitness functions are considered within 4% for all population members to guide next steps towards optimal design solutions. The best member of the current population

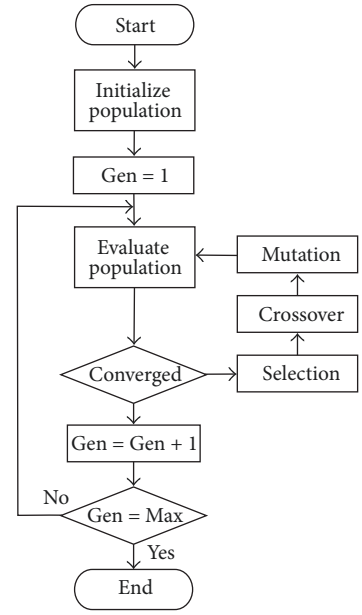

Figure 4: Flow chart of GA optimization process.

is alive and gains higher probability of reproduction, which will form a new offspring. It is the best solution that improves individual genetic characteristics generation until the optimal fitness set is obtained.

In the selection part, multiple population members are chosen at random conditions to produce the best one based on their fitness functions. The hypothetical individuals with higher fitness are reproduced by processes of crossover and mutation to generate the new offspring. Repetition of the processes brings about evolutionary population that strengthens their fitness function. After selecting one out of three members, the process repeats until the number of selected members matches the population size. Then the mating mechanism manipulates the genomes of the parent based on crossover stage. Firstly, the two selected members create two members of the new population. Then, two members are added to create the next generation under a defined crossover limit. Since the crossover operation, the algorithm of mutation allows for the possibility that some alternatives of the available population in the initial randomly can be represented within a mutation limit set. The mutation rate uses 1% in the GA arithmetic process as shown in Figure 4.

The procedure of the generic multiobjective GA is given as follows.

Step 1. Generate a random initialized population.

Step 2. For each objective Gen, Gen $= 1, 2, \ldots, k$, generate a random number and weight for each objective.

Step 3. Evaluate the fitness of the solution in the sorted population and calculate the selection probability of each solution.

Table 3: Comparison between original and optimized parameters of the LSA suspension, mm.

Design variables	y_A	z_A	y_C	z_C	y_D	z_D	y_F	z_F	y_G	z_G
Original	196.2	−134.3	196.2	−134.3	261.5	75.7	261.5	75.7	574.2	−80
Optimized	205.2	129.3	205.2	129.3	260.5	74.7	260.5	74.7	575.2	−75

Step 4. Select parents using the selection probabilities in Step 3.

Step 5. Apply the crossover on the selected parent pairs to create new offspring.

Step 6. Mutate the offspring created in Step 5 with a prespecified mutation rate and put all the offspring into the new population.

Step 7. If the stopping condition (Gen = Max) is not satisfied, set Gen = Gen + 1 and go to Step 3. Otherwise, end the procedure.

3.2. GA Optimizing Suspension Model. The aim is to find the optimal coordinates of hardpoints which are the key locations to influence on suspension characteristics according to their relative orientations. The design procedure accomplishes a suitable compromise between resolution accuracy and computational speed. In order to investigate the effect of geometry changes on suspension displacement limited to its free travel, the vertical and lateral direction of five hardpoints (A, C, D, F, and G) are selected as optimization variables and encoded into a binary string with fixed length.

The length of whole chromosome string has eight bits in GA optimization solution process because eight bits correspond to each value of parameter, y_A, z_A, y_C, z_C, y_D, z_D, y_F, z_F, y_G, and z_G, respectively.

For example, S_1 represents 00100100 which means the corresponding decimal values given as

$$y_A = X_{y_A\min} + \frac{d_{y_A}}{2^8 - 1}\left(X_{y_A\min} - X_{y_A\max}\right), \tag{5}$$

where $X_{y_A\min}$ and $X_{y_A\max}$ are the limit range for the coordinates of hardpoint y_A and d_{y_A} represents the binary value for S_1.

The aim of the optimization work is to minimize the sum of dynamic changes of wheel alignments. The design variations of hardpoint positions could be performed for geometry constrains and multiobjective optimizations.

After the preceding analysis, a GA optimization program is compiled and verified via implementation of virtual simulations. The block diagram representation of the GA operation process is given in Figure 5 with the aim of reaching minimum error. To correspond with the actual demand for the variation ranges in the wheel alignments and LAS suspension system, the corresponding original and optimized values of hardpoint positions are shown in Table 3.

3.3. Performance Analysis with Time Delay. When the constraints in multiobjective optimizations are activated, the

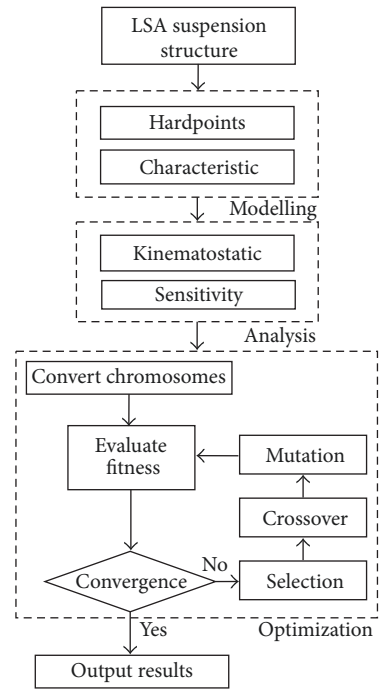

Figure 5: Block diagram of GA optimization program.

suspension system parameters, such as spring constant and damping coefficient, need to reconsider the effect of time delay on dynamic behavior due to the distance of front and rear axles (wheelbase) and different velocity.

The dynamic behavior can be correctly simulated by taking into account the value of time delay caused by the road excitations at the front and rear axles

$$q_f(t) = q_r(t + \tau), \tag{6}$$

where $q_f(t)$ and $q_r(t)$ are displacement excitations at front and rear axles, respectively, and τ means time delay, which can be calculated as follows:

$$\tau = \frac{(a + b)}{v}, \tag{7}$$

where a and b are the distance of mass center from front and rear axle, separately, and v represents vehicle speed.

The parameters of vehicle are summarized in Table 4.

The white noise disturbance that generates normally distributed random numbers, such as a sequence, feeds the input of nonlinear time delay model with the following set of parameters: noise power (the road roughness coefficient) $P = 256 \times 10^{-6}$ and sample time $T_e = 0.01$ s.

For the value of time delay, corresponding velocity of vehicle is computed by (7). $v_h = 80$ km/h indicates $\tau_1 =$

Table 4: Specification of the selected suspension system.

m_s kg	m_u kg	k_s N/m	k_t N/m	C_s N s/m	a m	b m
240	36	16000	160000	1400	1.2	1.3

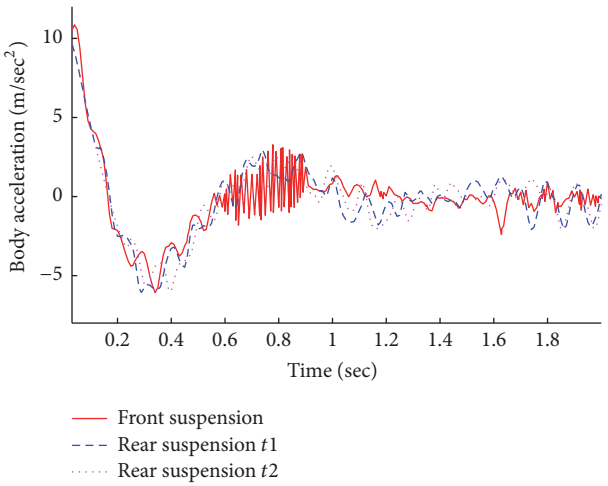

Figure 6: Time history of the body acceleration with different values of time delay.

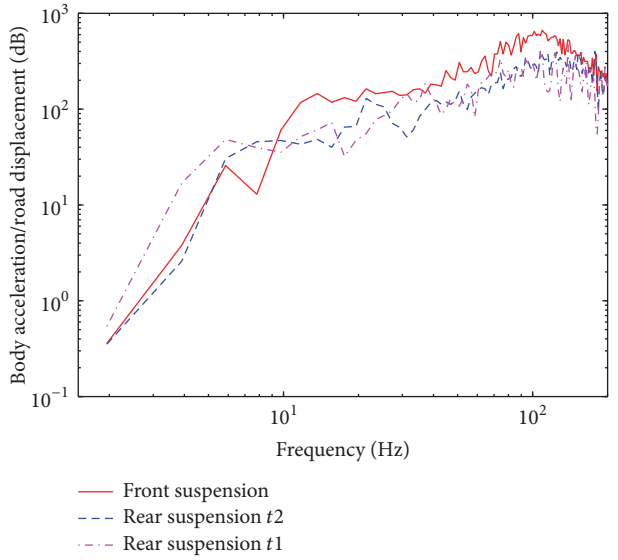

Figure 7: Frequency responses road displacement to body vertical acceleration.

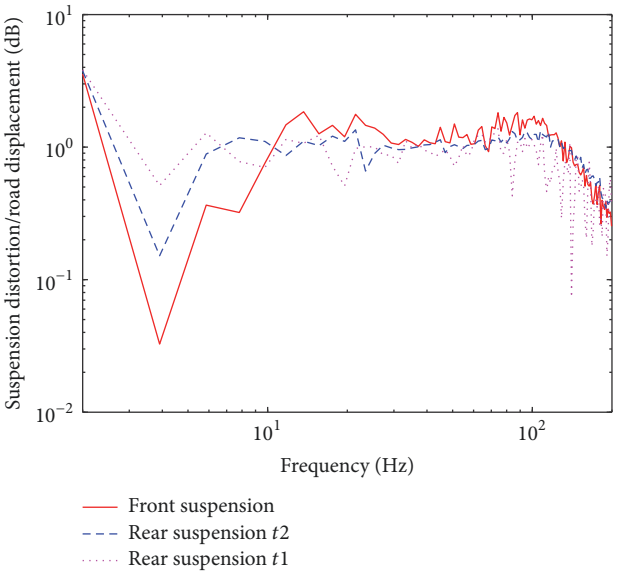

Figure 8: Frequency responses road displacement to suspension distortion.

0.1125 s and v_l = 40 km/h means τ_2 = 0.225 s. The effects of different time delay are shown in Figure 6. The time delay is not a constant but varies with the vehicle speed and the road roughness coefficient. The variation of frequency characteristic is activated to diminish time delay that is followed by increasing vehicle speed. It is obvious that vehicle body acceleration increases with time delay, which deteriorates ride comfort of the driver.

The frequency response analyses from the road displacement to the body vertical acceleration and suspension distortion are obtained by high vehicle speed and low vehicle speed as in Figures 7 and 8.

At low frequency, suspension provides a satisfied damping of the body vertical acceleration, but a bad filter of mid and high frequencies. On the other hand, a high time delay ensures a good filtering but a badly damped body vertical acceleration.

3.4. Simulation and Experiment. To correspond with the kinematics simulation analysis, the double-wishbone type suspension is designed with understeer characteristics. The simulation and experimental curves are illustrated in comparison with original and optimization toe and camber of the front suspension travel in Figures 9 and 10.

The camber angle decreases from 1.152° to 1.05° and toe-in angle reduces from 1.036° to 0.944°. The nonlinear suspension system with different values of time delay is investigated by numerical simulation. The travel displacements from −30 mm to 30 mm are utilized on front-right suspension. In Figure 9, it has been proved that the typical toe-out characteristics with a negative camber angle are beneficial to maintain the track path. The toe angle has a tendency with relatively small variation, which improves the steering response and road feeling at different suspension travels. As shown in Figure 10, the comparison with camber angle of original and optimization coordinates is obtained with the tire bouncing from the lowest position to the highest position. The two curves of camber angle are fitted well except for two ends of the suspension travel. The negative

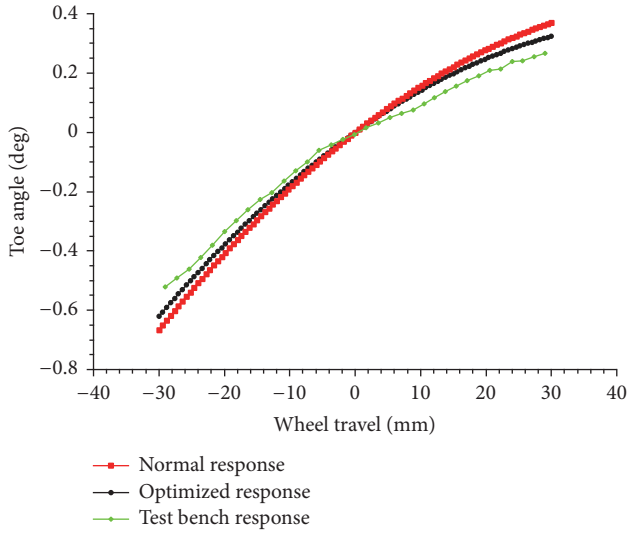

Figure 9: Block diagram of GA operation on LSA suspension and steering mechanism.

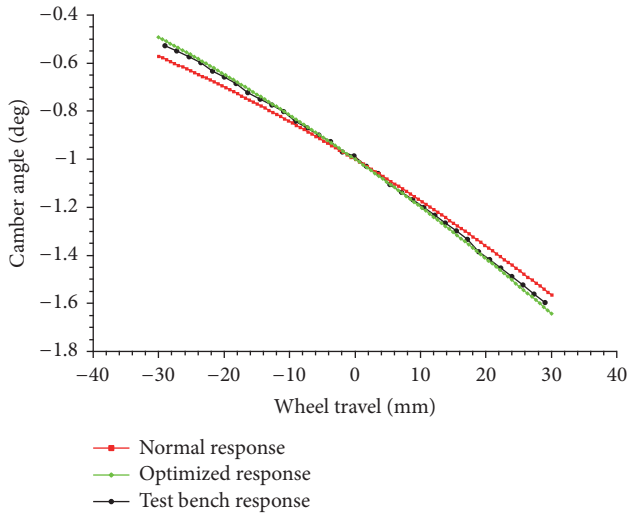

Figure 10: Block diagram of GA operation on LSA suspension and steering mechanism.

camber angle is the biggest contributor to keeping the vehicle on its straight-line path. At the compression and extension processes of suspension motion, the curves clearly indicate the hysteresis characteristic model of suspension with the optimization coordinates of hardpoint. Also there are more desirable characteristics for vehicle driving steerability than before.

The kinematics and compliance (K&C) facility is constructed with optical autocollimator sensors that are used to measure the toe and camber angle, amplifiers, and data acquisition systems to record the values in the whole test course. The test bench mainly consists of six hydraulic actuators to generate longitudinal, lateral, and vertical forces on two wheels with one axle, as shown in Figure 11. Because of the compliance steer forces, elastic bushing elements and

Figure 11: Kinematics and compliance test bench.

motions between the tire and road surface in the simulation are different from the real test bench. The influence of wheel travels on front suspension is taken into account which is essential for performing the experiment of actual working situations. The similarity of both simulation and testing curves is in very good agreement with the extremes of wheel.

4. Conclusions

By using multibody simulation tool, the double-wishbone type suspension (LSA) system has been built up for measuring values of the geometry and kinematic qualities. The sensitivity analysis process has been derived from a nonlinear computer model in order to optimize the principal design variables of main hardpoints. Consequently, the suspension model was simulated under certain driving conditions with optimized values and different values of time delay. The GA optimal solutions have been tested and modification of coefficients was repeated for the elastic elements, such as the spring stiffness and damper. It is necessary that the computer model and prototype have been obtained to validate effectiveness of the proposed method. The simulation and computational procedure can be applied to design an optimization problem of any other kind of suspension systems.

Conflicts of Interest

The authors declare that there are no conflicts of interest regarding the publication of this manuscript.

Acknowledgments

This research work was supported by International Science & Technology Cooperation Program of China (2013DFA31920), the National Key Research and Development Program of China (2017YFD0401304), and the National Natural Science Foundation of China (Grant no. 51476143).

References

[1] M. Heidari and H. Homaei, "Design a PID controller for suspension system by back propagation neural network," *Journal of Engineering*, vol. 2013, Article ID 421543, pp. 1–9, 2013.

[2] C. Tan, R. Xu, Z. Wang, L. Si, and X. Liu, "An improved genetic fuzzy logic control method to reduce the enlargement of coal floor deformation in shearer memory cutting process," *Computational Intelligence and Neuroscience*, vol. 2016, Article ID 3973627, pp. 1–14, 2016.

[3] D. Özcan, Ü. Sönmez, and L. Güvenç, "Optimisation of the nonlinear suspension characteristics of a light commercial vehicle," *International Journal of Vehicular Technology*, vol. 2013, Article ID 562424, pp. 1–16, 2013.

[4] A. Seifi, R. Hassannejad, and M. A. Hamed, "Use of nonlinear asymmetrical shock absorbers in multi-objective optimization of the suspension system in a variety of road excitations," *Proceedings of the Institution of Mechanical Engineers, Part K: Journal of Multi-body Dynamics*, vol. 231, no. 2, pp. 372–387, 2017.

[5] V. Savsani, V. Patel, B. Gadhvi, and M. Tawhid, "Pareto optimization of a half car passive suspension model using a novel multiobjective heat transfer search algorithm," *Modelling and Simulation in Engineering*, vol. 2017, Article ID 2034907, pp. 1–17, 2017.

[6] V. Mehta, M. Patel, Y. Gandhi, and B. Gadhvi, "An experimental approach of estimating speed bump profile to optimizing the suspension parameters using TLBO," *Journal of Advances in Vehicle Engineering*, vol. 2, no. 2, pp. 65–74, 2016.

[7] A. Jamali, H. Shams, and M. Fasihozaman, "Pareto multi-objective optimum design of vehicle-suspension system under random road excitations," *Proceedings of the Institution of Mechanical Engineers, Part K: Journal of Multi-body Dynamics*, vol. 228, no. 3, pp. 282–293, 2014.

[8] T. Tak, S. Chung, and H. Chun, "An optimal design software for vehicle suspension systems," SAE Technical Papers 2000-01-1618, 2000.

[9] K.-H. Suh, Y.-K. Lee, and H.-M. Jeong, "A study on the handling performances of a large-sized bus with the change of rear suspension geometry," SAE Technical Papers 2002-01-3071, 2002.

[10] J. Park, J. Yi, and D. Lee, "Investigation into suspension dynamic compliance characteristics using direct measurement and simulation," SAE Technical Papers 2004-01-1065, 2004.

[11] H.-S. Kim, W.-J. Do, J.-S. Shim, and S.-R. Choi, "The stability analysis of steering and suspension parameters on hands free motion," SAE Technical Papers 2002-01-0620, 2002.

[12] S. A. Mitchell, S. Smith, A. Damiano, J. Durgavich, and R. MacCracken, "Use of genetic algorithms with multiple metrics aimed at the optimization of automotive suspension systems," SAE Technical Papers 2004-01-3520, 2004.

[13] K. Deb, A. Pratap, S. Agarwal, and T. Meyarivan, "A fast and elitist multiobjective genetic algorithm: NSGA-II," *IEEE Transactions on Evolutionary Computation*, vol. 6, no. 2, pp. 182–197, 2002.

[14] B. Gadhvi, V. Savsani, and V. Patel, "Multi-objective optimization of vehicle passive suspension system using NSGA-II, SPEA2 and PESA-II," *Procedia Technology*, vol. 23, pp. 361–368, 2016.

[15] A. C. Mitra, G. J. Desai, S. R. Patwardhan, P. H. Shirke, W. M. H. Kurne, and N. Banerjee, "Optimization of passive vehicle suspension system by genetic algorithm," *Procedia Engineering*, vol. 144, pp. 1158–1166, 2016.

[16] J. Yan, Z. Yin, X. Guo, and C. Fu, "Fuzzy control of semi-active air suspension for cab based on genetic algorithms," SAE Technical Papers 2008-01-2681, 2008.

[17] S. Hasagasioglu, K. Kilicaslan, O. Atabay, and A. Güney, "Vehicle dynamics analysis of a heavy-duty commercial vehicle by using multibody simulation methods," *The International Journal of Advanced Manufacturing Technology*, vol. 60, no. 5-8, pp. 825–839, 2012.

[18] K. Abdullah, W. C. David, and E. S. Alice, "Multi-objective optimization using genetic algorithms: a tutorial," *Reliability Engineering & System Safety*, vol. 91, no. 9, pp. 992–1007, 2006.

[19] N. Srinivas and K. Deb, "Multiobjective optimization using non-dominated sorting in genetic algorithms," *Evolutionary Computation*, vol. 2, no. 3, pp. 221–248, 1995.

[20] R. Darvishi, M. N. Esfahany, and R. Bagheri, "Numerical study on increasing PVC suspension polymerization productivity by using PSO optimization algorithm," *International Journal of Plastics Technology*, vol. 20, no. 2, pp. 219–230, 2016.

[21] J. Wu, Z. Luo, Y. Zhang, and N. Zhang, "An interval uncertain optimization method for vehicle suspensions using Chebyshev metamodels," *Applied Mathematical Modelling*, vol. 38, no. 15-16, pp. 3706–3723, 2014.